Advances in Nano Research, *Vol. 7 No. 4 (2019) 223-231*
DOI: https://doi.org/10.12989/anr.2019.7.4.223

Vibration analysis of magneto-flexo-electrically actuated porous rotary nanobeams considering thermal effects via nonlocal strain gradient elasticity theory

Farzad Ebrahimi [*1], Mahsa Karimiasl [1] and Vinyas Mahesh [2,3]

[1] *Department of Mechanical Engineering, Faculty of Engineering, Imam Khomeini International University, Postal code: 3414916818, Qazvin, Iran*
[2] *Department of Aerospace Engineering, Indian Institute of Science, Bangalore, India*
[3] *Department of Mechanical Engineering, Nitte Meenakshi Institute of Technology, Bangalore,560064 India*

(*Received February 2, 2018, Revised April 3, 2019, Accepted June 4, 2019*)

Abstract. In this article the frequency response of magneto-flexo-electric rotary porous (MFERP) nanobeams subjected to thermal loads has been investigated through nonlocal strain gradient elasticity theory. A quasi-3D beam model beam theory is used for the expositions of the displacement components. With the aid of Hamilton’s principle, the governing equations of MFERP nanobeams are obtained. Further, administrating an analytical solution the frequency problem of MFERP nanobeams are solved. In addition the numerical examples are also provided to evaluate the effect of nonlocal strain gradient parameter, hygro thermo environment, flexoelectric effect, in-plane magnet field, volume fraction of porosity and angular velocity on the dimensionless eigen frequency.

Keywords: eigenfrequency; angular velocity; volume fraction of porosity; FG nanobeam; Visco-Pasternak foundation

1. Introduction

Functionally Graded Material (FGM) is one of the materials that exhibit different properties in different regions due to the gradual change in the chemical composition, distribution, orientation, or size of the reinforcing phase in one or more dimensions. This gradual change in structure and properties has led to the expansion of its use in various domains. Considering the various applications of these materials in the air, military and defense industries, the study of methods and techniques for making these materials is important and necessary. Therefore, the hygro-thermal analysis of FGM structures is a benefit case in research .The nonlocal continuum mechanics theories in contrast to classical theory emphasize that the stress at a point is not just directed to a point, but also depends on other points. Meanwhile, in the classical theory, stress is limited to a single point as expressed by Eringen (1968, 1972). Following the Eringen’s theory, many studies have been carried out to highlight some of important issues: The postbuckling analysis of FG beams in micro scales under thermal loading is investigated by Ghorbanpour Arani *et al*. (2015). The buckling behaviour of piezoelectric FG beams under thermal and electric loading was studied by Kiani *et al*. (2011). Rahmani and Jandaghian (2015) researched the mechanical response of FG beam theory through third-order shear deformation via nonlocal theory. Yang *et al*. (2010) studied nonlinear vibration of single walled carbon nanotubes (SWCNTs). Based on the elastic medium the stability responses of SWCNT were described. The effect of Winkler and Pasternak parameter, aspect ratio of the SWCNT and nonlocal parameter were also studied in their research. The vibration and buckling characteristics of piezoelectric and piezomagnetic nano-beams based on various beam models was verified by Ebrahimi and Barati (2016a, b, c, d, 2017). In their research, the electro-magnetic effect of piezoelectric materials has been investigated and also the mechanical responses of FGM nanobeams have been observed under various significant parameters. They realized that the effect of the electro-magnetic hygrothermal loading increases the dimensionless frequency and buckling load. The vibration, buckling and bending behaviour of Timoshenko nanobeams based on meshless method was investigated by Roque *et al*. (2011). Embedded in the nonlocal component relevance of Eringen, major of articles were published searching to extend the nonlocal beam models for nano structures. Peddieson *et al*. (2003) proposed nonlocal Euler–Bernoulli and Timoshenko beam theory whose credibility to predict bending behaviour was accepted and verified by many studies (Civalek and Demir 2011, Wang 2005, Wang *et al*. 2008). During the years of research, the small-size effects in SWCNTs studied by Murmu and Pradhan (2009). Thermo-magneto-electro-elastic analysis of a functionally graded nanobeam integrated with functionally graded piezo-magnetic layers was studied by Arefi (Arefi and Zenkour 2016). Zenkour and Sobhy (2013) studied the thermal buckling analysis of single-layered graphene sheets lying on an elastic medium. Bending of Electro-mechanical sandwich nanoplate based on silica Aerogel foundation examined by Ghorbanpour Arani *et al*. (2017). The

∗Corresponding author, Professor,
E-mail: febrahimy@ut.ac.ir

http://www.techno-press.org/?journal=journal=anr&subpage=5
ISSN: 2287-237X (Print), 2287-2388 (Online)

influence of parameters such as applied voltage, porosity index, foundation parameter, aspect ratio on the bending response of sandwich nanoplates was studied. Şimşek and Yurtcu (2013) presented the bending analysis of shear and normal deformations beam theory based on nonlocal theory.

In this article, vibration characteristics of MFERP nanobeams based on quasi-3D beam model theory. The governing equations used by Hamilton principle and are solved by analytical method. The effects of various parameters such as flexoelectric effect, nonlocal and strain gradient parameter, power-law index and Winkler Visco-Pasternak foundation on dimensionless frequency are researched.

2. Materials and methods

2.1 The material properties of MFERP nanobeam

A MFERP nanobeam with thickness (h) and length (L) illustrate in Fig. 1. The properties of MFERP nanobeam ($BaTiO_3$,$CoFe_2O_4$) shown in Table 1. (Ke and Wang 2014)

Regarding porosity volume fraction has

$$P_f = P_c V_c + P_m V_m + \frac{\alpha}{2}(P_c - P_m) \tag{1}$$

P_m and P_c consider metal and ceramic material properties, respectively; and stands for the volume fraction of porosity express by α, while, V_c and V_m are the volume fractions of ceramic and metal phases, respectively, the relation can be written by

$$V_c + V_m = 1 \tag{2}$$

The volume fraction of ceramic phase can be calculated in any desired thickness express by

$$V_c = \left(\frac{z}{h} + \frac{1}{2}\right)^p \tag{3}$$

Now, substituting Eqs. (2) and (3) in Eq. (1) results in an equation for equivalent material properties of porous FG beam

$$P(z) = (P_c - P_m)\left(\frac{z}{h} + \frac{1}{2}\right)^p + P_m + \frac{\alpha}{2}(P_c - P_m) \tag{4}$$

2.2 Kinematic relations

A quasi-3D beam model accounting for shear deformation is considred. The displacement can be written as

$$u_1(x,y,z) = u(x,y) - z\frac{\partial w_b}{\partial x} - f(z)\frac{\partial w_s}{\partial x} \tag{5}$$

$$u_2(x,y,z) = v(x,y) - z\frac{\partial w_b}{\partial y} - f(z)\frac{\partial w_s}{\partial y} \tag{6}$$

$$u_3(x,y,z) = w_b(x,y) + w_s(x,y) + g(z)w_z(x,y) \tag{7}$$

in which u, v, w_b, w_s and w_z are unknowns of displacements of mid-plane. Also, $f(z)$ is a shape function that determines. The present theory has a function in the form

$$f(z) = z - \sin(\xi z)/\xi \tag{8}$$

Also, the Hamilton's principle states that

$$\int_0^t \delta(\Pi_S - \Pi_K + \Pi_W)\mathrm{d}t = 0 \tag{9}$$

where Π_S is the total strain energy and external applied forces denote by Π_W. The strain energy variation Π_S can be computed as

$$\delta\Pi_S = \int \sigma_{ij}\delta\varepsilon_{ij}dv = \int \sigma_x\delta\varepsilon_x + \sigma_{xz}\delta\gamma_{xz} + \sigma_{yz}\delta\gamma_{yz} \tag{10}$$

Substituting Eqs.(5) - (7) into Eq.(9) yields

$$\begin{aligned}\delta\Pi_S = \int_0^l (N\frac{\partial\delta u}{\partial x} - M_b\frac{\partial^2\delta w_b}{\partial x^2} \\ -M_s\frac{\partial^2\delta w_s}{\partial x^2} + Q\frac{\partial\delta w_s}{\partial x})dx\end{aligned} \tag{11}$$

In which the variables at the last expression are expressed by

$$\{Ni, Mi\} = \int_{-h/2}^{h/2} \sigma_i\{1, z^2\}\mathrm{d}z\,, i = (x, y, xy) \tag{12}$$

In this study, the nanobeam is subjected to an in-plane axial magnetic field. Hence, to derive the exerted body force from longitudinal magnetic field H = (H_x, 0, 0), the Maxwell relations are adopted

$$f_{Lz} = \eta(\nabla\times(\nabla\times(\vec{u}\times\vec{H})))\times\vec{H} \tag{13}$$

Where $\vec{u} = (u_x, 0, u_z)$ is displacement vector and η is magnetic parliamentary. For a planar beam deformation with the assumed displacement field, the resultant Lorentz force takes the form

$$f_{Lz} = \eta\int_A f_z dA = \eta A H_x^2\frac{\partial^2 w}{\partial x^2} \tag{14}$$

The variation of the work can be written in the form

Table 1 Piezo-electro-elastic coefficients of material properties

Properties	$BaTiO_3$	$CoFe_2O_4$
c_{11} (GPa)	166	286
e_{31} (Cm^{-2})	-4.4	0
k_{11} ($10^{-9}C^2m^{-2}N^{-1}$)	11.2	0.08
k_{13}	12.6	0.093
ρ (kgm^{-3})	5800	5300

$$\delta\Pi_w = \int_0^a \left[\left(-N_x^0 \frac{\partial w^b}{\partial x}\frac{\partial \delta w^b}{\delta x} - k_w \delta(w^b + w^s)\right.\right.$$
$$\left. + k_p \partial^2 \frac{(w_{b+} w_{s)}}{\partial x^2}\right] dx - c_d \frac{\partial \delta(w^b + w^s)}{\delta t} \tag{15}$$
$$-\eta A H_x^2 \frac{\partial^2 \delta(w^b + w^s)}{\partial x^2} + f_{13}\delta(w^b + w^s)$$

where f_{13}, N^T, N^R are flexoelectricity coefficient, applied forces due to variation of temperature and beam's angular velocity around the z axis, respectively, and can be defined in the following form as

$$\mathrm{N^R} = \int_x^L \int_A (\rho(z)\mathrm{A}\Omega^2 x)\mathrm{dA\,dx}$$
$$N^T = b\int_{-h/2-h_0}^{\frac{h}{2}-h_0} (\alpha\,\Delta T)dz \tag{16}$$

where Ω denotes the angular velocity of the nanobeam. In this research the maximum amount of the axial force generated by the rotation of the beam is considered as follows

$$\mathrm{N^R_{max}} = \int_0^L \int_A (\rho(z)\mathrm{A}\Omega^2 x)\mathrm{dA\,dx} \tag{17}$$

where $\Delta T = T - T_0$ in which T_0 is the reference temperature concentration, respectively and k_w Winkler coefficient, k_p and c_d are shear and damping coefficients of medium, respectively. The variation of kinetic energy is represented by

$$\delta\Pi_k = \int_0^l I_0 \left[\frac{\partial u}{\partial t}\frac{\partial \delta u}{\partial t} + \left(\frac{\partial w_b}{\partial t} + \frac{\partial \delta w_s}{\delta t}\right)\left(\frac{\partial w_b}{\partial t} + \frac{\partial \delta w_s}{\delta t}\right)\right.$$
$$-I_1\left(\frac{\partial u}{\partial t}\frac{\partial^2 \delta w_b}{\partial x \partial t} + \frac{\partial \delta u}{\partial t}\frac{\partial^2 w_b}{\delta x \partial t}\right)$$
$$\left. + I_2\left(\frac{\partial^2 w_b}{\partial x \partial t}\frac{\partial^2 \delta w_b}{\partial x \partial t}\right)\right]$$
$$-J_1\left(\frac{\partial u}{\partial t}\frac{\partial^2 \delta w^s}{\partial x \partial t} + \frac{\partial \delta u}{\partial t}\frac{\partial^2 w_s}{\delta x \partial t}\right) \tag{18}$$
$$+K_2\left(\frac{\partial^2 w_s}{\partial x \partial t}\frac{\partial^2 \delta w_s}{\partial x \partial t}\right)$$
$$+J_2\left(\frac{\partial^2 w_b}{\partial x \partial t}\frac{\partial^2 \delta w_s}{\partial x \partial t} + \frac{\partial^2 w_s}{\partial x \partial t}\frac{\partial^2 \delta w_b}{\partial x \partial t}\right)$$

where

$$(I_0, I_1, J_1, I_2, J_2, K_2) = \int_{-h/2-h_0}^{h/2-h_0} \rho(z_{ns})(1, z_{ns}, f, z_{ns}^2, z_{ns} f, f^2)dz_{ns} \tag{19}$$

The governing equations are obtained by inserting Eqs. (10)-(15) in Eq. (9) when the coefficients of δu, δw_b and δw_s are equal to zero

$$\frac{\partial N}{\partial x} = I_0 \frac{\partial^2 u}{\partial t^2} - I_1 \frac{\partial^3 w_b}{\partial x \partial t^2} - J_1 \frac{\partial^3 w_s}{\partial x \partial t^2} \tag{20}$$
$$-\eta A H_x^2 (w^b + w^s)$$

$$\frac{\partial^2 M_b}{\partial x^2} + (N^R - N^T + Kp)\nabla^2(w^b + w^s)$$
$$-I_0\left(\frac{\partial^2 w_b}{\partial t^2} + \frac{\partial^2 w_s}{\partial t^2}\right) - I_1 \frac{\partial^3 u}{\partial x \partial t^2} + I_2 \frac{\partial^4 w_b}{\partial x^2 \partial t^2} \tag{21}$$
$$-k_w(w^b + w^s) + c_d \frac{\partial (w_b + w_s)}{\partial t} = 0$$

$$\frac{\partial^2 M_b}{\partial x^2} + \frac{\partial Q}{\partial x} + (N^R - N^T + Kp)\nabla^2(w^b + w^s)$$
$$-I_0\left(\frac{\partial^2 w_b}{\partial t^2} + \frac{\partial^2 w_s}{\partial t^2}\right) - J_1 \frac{\partial^3 u}{\partial x \partial t^2} + J_2 \frac{\partial^4 w_b}{\partial x^2 \partial t^2} \tag{22}$$
$$+k_2 \frac{\partial^4 w_s}{\partial x^2 \partial t^2} - k_w(w^b + w^s) + c_d \frac{\partial (w_b + w_s)}{\partial t} = 0$$

2.3 Elasticity theory of nonlocal strain gradient of MFERP nanobeams

The important role of the nonlocal strain gradient elasticity theory is that the nonlocal stress tensor at a reference point relies on the strain tensor of the same coordinate and on other points in the solid.

$$\sigma_{ij} = \sigma_{ij}^{(0)} - \frac{d\sigma_{ij}^{(1)}}{dx} \tag{23}$$

Where the stress $\sigma_{xx}^{(0)}$ corresponds to strain ε_{xx} and higher order stress $\sigma_{xx}^{(1)}$ corresponds to strain gradient $\varepsilon_{xx,x}$ and are defined by

$$\sigma_{ij}^{(0)} = \int_0^L C_{ijkl}\alpha_0(x, x', e_0 a)\varepsilon'_{kl}(x')dx' \tag{24a}$$

$$\sigma_{ij}^{(1)} = l^2 \int_0^L C_{ijkl}\alpha_1(x, x', e_1 a)\varepsilon'_{kl,x}(x')dx' \tag{24b}$$

In which C_{ijkl} are the elastic constants and e_0a and e_1a consider the influences of nonlocal stress field, and l denote the material length scale parameter and captures the effects of higher-order strain gradient stress field. The relation for a MFERP nanobeam can be stated as

$$[1-(e_1 a)^2\nabla^2][1-(e_0 a)^2\nabla^2]\sigma_{ij}$$
$$= C_{ijkl}[1-(e_1 a)^2\nabla^2]\varepsilon_{kl} - C_{ijkl}\, l^2[1-(e_0 a)^2\nabla^2]\nabla^2\varepsilon_{kl} \tag{25a}$$

In which ∇^2 denotes the Laplacian operator. Supposing $e_1 = e_0 = e$ and discarding terms of order $O(\nabla^2)$, the general constitutive relation in Eq. (25a) can be rewritten as

$$[1-(ea)^2\nabla^2]\sigma_{ij} = C_{ijkl}[1-l^2\nabla^2]\varepsilon_{kl} \tag{25b}$$

Also

$$\sigma_{ij-}(ea)^2\nabla^2\sigma_{ij} = 1 - l^2\nabla^2\left[C_{ijkl}\varepsilon_{kl} - f_{klij}\frac{\partial_{E_K}}{\partial x_l} + C_{ijkl}\alpha_{kl}\right] \tag{26}$$

where α_{ij} and β_{ij} are thermal and moisture expansion coefficients, respectively; Thus, the communicate relations MFERP nanobeam can be stated as

$$\sigma_{xx} - \mu\frac{\partial^2\sigma_{xx}}{\partial x^2} = E(Z_{ns})\left(\varepsilon_{xx} - \eta\frac{\partial^2\varepsilon_{xx}}{\partial x^2} - \alpha\Delta T - f_{lz}\right) \tag{27a}$$

$$\sigma_{xz} - \mu\frac{\partial^2\sigma_{xz}}{\partial x^2} = G(Z_{ns})\left(\gamma_{xz} - \eta\frac{\partial^2\gamma_{xz}}{\partial x^2}\right) \tag{27b}$$

where $\mu = ea^2$ and $\eta = l^2$. Applying the Kelvin's model on elastic materials with viscoelastic structural damping coefficient (g) and integrating Eq. (28) over the cross-section area of nanobeam provides the following nonlocal relations for a refined beam model as

$$N - \mu\frac{\partial^2 N}{\partial x^2} = \left(1 - \eta\frac{\partial^2}{\partial x^2}\right)\left(1 + g\frac{\partial}{\partial t}\right)\left(A\frac{\partial u}{\partial x} - B\frac{\partial^2 w_b}{\partial x^2} - B_S\frac{\partial^2 w_s}{\partial x^2}\right) - N_x^T - N_{max}^R \tag{28}$$

$$M_b - \mu\frac{\partial^2 M_b}{\partial x^2} = \left(1 - \eta\frac{\partial^2}{\partial x^2}\right)\left(1 + g\frac{\partial}{\partial t}\right)\left(B\frac{\partial u}{\partial x} - D\frac{\partial^2 w_b}{\partial x^2} - D_S\frac{\partial^2 w_s}{\partial x^2}\right) - M_x^T \tag{29}$$

$$M_S - \mu\frac{\partial^2 M_S}{\partial x^2} = \left(1 - \eta\frac{\partial^2}{\partial x^2}\right)\left(1 + g\frac{\partial}{\partial t}\right)\left(B_S\frac{\partial u}{\partial x} - D_S\frac{\partial^2 w_b}{\partial x^2} - H_s\frac{\partial^2 w_s}{\partial x^2}\right) - M_x^T \tag{30}$$

$$Q - \mu\frac{\partial^2 Q}{\partial x^2} = \left(1 - \eta\frac{\partial^2}{\partial x^2}\right)\left(1 + g\frac{\partial}{\partial t}\right)\left(A_s\frac{\partial w_s}{\partial x}\right) \tag{31}$$

where the cross-sectional rigidities are calculated as follows

$$(A, B, B_s, D, D_s, H_s) = \int_{-h/2-h_0}^{h/2-h_0} E(z_{ns})(1, z_{ns}, f, z_{ns}{}^2, z_{ns}f, f^2)\,dz_{ns} \tag{32}$$

$$A_s = \int_{-h/2-h_0}^{h/2-h_0} g^2 G(z_{ns})dz_{ns} \tag{33}$$

$$\{N_x^T, M_b^T, M_s^T\} = \int_{-\frac{h}{2}-h_0}^{\frac{h}{2}-h_0} E(z_{ns})\alpha(z_{ns})(T - T_0)\{1, z_{ns}, f\}dz_{ns} \tag{34}$$

Displacements of MFERP nanobeam are illustrated by inserting for M_b, M_s, Q and N from Eqs. (29)-(32), respectively into Eqs. (20)-(22) as follows

$$\begin{aligned}
&A(1-\eta\frac{\partial^2}{\partial x^2})(\frac{\partial^2 u}{\partial x^2} + g\frac{\partial^3 u}{\partial t\partial x^2}) \\
&- B(1-\eta\frac{\partial^2}{\partial x^2})(\frac{\partial^3 w_b}{\partial x^3} + g\frac{\partial^4 w_b}{\partial t\partial x^3}) \\
&- B_s(1-\eta\frac{\partial^2}{\partial x^2})(\frac{\partial^3 w_s}{\partial x^3} + g\frac{\partial^4 w_s}{\partial t\partial x^3}) \\
&- I_0\frac{\partial^2 u}{\partial t^2} + I_1\frac{\partial^3 w_b}{\partial x\partial t^2} + J_1\frac{\partial^3 w_s}{\partial x\partial t^2} \\
&+ \mu(I_0\frac{\partial^4 u}{\partial x^2\partial t^2} - I_1\frac{\partial^5 w_b}{\partial x^3\partial t^2} - J_1\frac{\partial^5 w_s}{\partial x^3\partial t^2}) = 0
\end{aligned} \tag{35}$$

$$\begin{aligned}
&B\left(1 - \eta\frac{\partial^2}{\partial x^2}\right)\left(\frac{\partial^3 u}{\partial x^3} + g\frac{\partial^4 u}{\partial t\partial x^3}\right) \\
&-D\left(1 - \eta\frac{\partial^2}{\partial x^2}\right)\left(\frac{\partial^4 w_b}{\partial x^4} + g\frac{\partial^5 w_b}{\partial t\partial x^4}\right) \\
&-D_s\left(1 - \eta\frac{\partial^2}{\partial x^2}\right)\left(\frac{\partial^4 w_s}{\partial x^4} + g\frac{\partial^5 w_s}{\partial t\partial x^4}\right) \\
&+A_S\left(1 - \eta\frac{\partial^2}{\partial x^2}\right)\left(\frac{\partial^2 w_s}{\partial x^2} + g\frac{\partial^3 w_s}{\partial t\partial x^2}\right) \\
&-I_0\left(\frac{\partial^2 w_b}{\partial t^2} + \frac{\partial^2 w_s}{\partial t^2}\right) - I_1\frac{\partial^3 u}{\partial x\partial t^2} + I_2\frac{\partial^4 w_b}{\partial x^2\partial t^2} \\
&+J_2\frac{\partial^4 w_s}{\partial x^2\partial t^2} - k_w(w_b + w_s) - \eta A H_x^2(w^b + w^s) \\
&] + k_p\frac{\partial^2(w_b + w_s)}{\partial x^2} - c_d\frac{\partial(w_b + w_s)}{\partial t} \\
&+\mu((N^T + N_{max}^R)\frac{\partial^4(w_b + w_s)}{\partial x^4} \\
&+I_0\left(\frac{\partial^4 w_b}{\partial x^2\partial t^2} + \frac{\partial^4 w_s}{\partial x^2\partial t^2}\right) + I_1\frac{\partial^3 u}{\partial x^3\partial t^2} - I_2\frac{\partial^6 w_b}{\partial x^4\partial t^2} \\
&+J_2\frac{\partial^6 w_s}{\partial 4\partial t^2} + k_w\frac{\partial^2(w_b + w_s)}{\partial x^2} + k_p\frac{\partial^4(w_b + w_s)}{\partial x^4} \\
&+\eta A H_x^2\frac{\partial^2(w_b + w_s)}{\partial x^2} + c_d\frac{\partial^3(w_b + w_s)}{\partial x^2\partial t} \\
&-\frac{e_{31}}{2k_{33}}f_{13}\left(\frac{\partial^2 w_b}{\partial x^2} + \frac{\partial^2 w_s}{\partial x^2}\right)
\end{aligned} \tag{36}$$

$$\begin{aligned}
&B_s(1 - \eta\tfrac{\partial^2}{\partial x^2})(\tfrac{\partial^3 u}{\partial x^3} + g\tfrac{\partial^4 u}{\partial t\partial x^3}) \\
&-D_s\left(1 - \eta\frac{\partial^2}{\partial x^2}\right)\left(\frac{\partial^4 w_b}{\partial x^4} + g\frac{\partial^5 w_b}{\partial t\partial x^4}\right) \\
&-H_s\left(1 - \eta\frac{\partial^2}{\partial x^2}\right)\left(\frac{\partial^4 w_s}{\partial x^4} + g\frac{\partial^5 w_s}{\partial t\partial x^4}\right) \\
&+A_S\left(1 - \eta\frac{\partial^2}{\partial x^2}\right)\left(\frac{\partial^2 w_s}{\partial x^2} + g\frac{\partial^3 w_s}{\partial t\partial x^2}\right) \\
&-I_0\left(\frac{\partial^2 w_b}{\partial t^2} + \frac{\partial^2 w_s}{\partial t^2}\right) - J_1\frac{\partial^3 u}{\partial x\partial t^2} + J_2\frac{\partial^4 w_b}{\partial x^2\partial t^2} \\
&+k_2\frac{\partial^4 w_s}{\partial x^2\partial t^2} - k_w(w_b + w_s) - \eta A H_x^2(w^b + w^s)
\end{aligned} \tag{37}$$

$$
\begin{aligned}
&+k_p \frac{\partial^2(w_b+w_s)}{\partial x^2} - c_d \frac{\partial(w_b+w_s)}{\partial t} \\
&+\mu((N^T+N_{max}^R)\frac{\partial^4(w_b+w_s)}{\partial x^4} \\
&+I_0\left(\frac{\partial^4 w_b}{\partial x^2 \partial t^2}+\frac{\partial^4 w_s}{\partial x^2 \partial t^2}\right)+J_1 \frac{\partial^3 u}{\partial x^3 \partial t^2}-J_2 \frac{\partial^6 w_b}{\partial x^4 \partial t^2} \\
&+k_2 \frac{\partial^6 w_s}{\partial 4 \partial t^2}+k_w \frac{\partial^2(w_b+w_s)}{\partial x^2}+k_p \frac{\partial^4(w_b+w_s)}{\partial x^4} \\
&+\eta A H_x^2 \frac{\partial^2(w_b+w_s)}{\partial x^2}+c_d \frac{\partial^3(w_b+w_s)}{\partial x^2 \partial t} \\
&-\frac{e_{31}}{2k_{33}} f_{13}\left(\frac{\partial^2 w_b}{\partial x^2}+\frac{\partial^2 w_s}{\partial x^2}\right)
\end{aligned} \tag{37}
$$

3. Solution procedure

In this section, an analytical solution is implemented in which the generalized displacements are expanded in a double Fourier series in terms of unknown parameters. The selection of the functions in these series is associated to those which satisfy the boundary edges of the nanoplate. These boundary edges are given as:

- Simply-supported (S):

$$w_b = w_s = N_x = M_x = 0 \qquad \text{at } x = 0, a \tag{38}$$

$$w_b = w_s = N_y = M_y = 0 \qquad \text{at } y = 0, b \tag{39}$$

- Clamped (C):

$$u = v = w_b = w_s = 0 \qquad x = 0, a \quad \text{and} \quad y = 0, b \tag{40}$$

To obtain boundary conditions we use the following equations

$$u(x,t) = \sum_{n=1}^{\infty} U_n \frac{\partial X_n(x)}{\partial x} e^{i\omega_n t} \tag{41}$$

$$v(x,t) = \sum_{n=1}^{\infty} V_n \frac{\partial X_n(x)}{\partial x} e^{i\omega_n t} \tag{42}$$

$$w_b(x,t) = \sum_{n=1}^{\infty} \mathrm{W}_{bn} X_n(x) e^{i\omega_n t} \tag{43}$$

$$w_s(x,t) = \sum_{n=1}^{\infty} \mathrm{W}_{sn} X_n(x) e^{i\omega_n t} \tag{44}$$

$$w_z(x,t) = \sum_{n=1}^{\infty} \mathrm{W}_{zn} X_n(x) e^{i\omega_n t} \tag{45}$$

where [K], [C] and [M] are the stiffness, damping, and mass matrixes for FG nanobeam, respectively.

$$
\begin{aligned}
&k_{1,1} = A(\alpha_3 - \eta\alpha_{11}), \\
&K_{1,2} = B(\alpha_9 - \eta\alpha_{13}), \\
&K_{1,3} = B_S(\alpha_9 - \eta\alpha_{13}) \\
&k_{2,3} = (N^T + N_{max}^R - k_p)(-\alpha_7 + \mu\alpha_9) - k_w(\alpha_5 - \mu\alpha_7) \\
&\qquad - f_{Iz}(\alpha_5 - \mu\alpha_7) - D_s(\alpha_9 - \eta\alpha_{13}) \\
&K_{2,2} = (N^T + N_{max}^R - k_p)(-\alpha_7 + \mu\alpha_9) - k_w(\alpha_5 - \mu\alpha_7) \\
&\qquad - f_{Iz}(\alpha_5 - \mu\alpha_7) - D(\alpha_9 - \eta\alpha_{13}) \\
&K_{3,3} = (N^T + N_{max}^R - k_p)(-\alpha_7 + \mu\alpha_9) - k_w(\alpha_5 - \mu\alpha_7) \\
&\qquad - A_s(\alpha_5 - \mu\alpha_7) - \frac{e_{31}}{2k_{33}} f_{13}(\alpha_5 - \mu\alpha_7) \\
&\qquad - H_s(\alpha_9 - \eta\alpha_{13}) \\
&c_{1,1} = Aig(\alpha_3 - \eta\alpha_{11}), \\
&c_{1,2} = Big(\alpha_9 - \eta\alpha_{13}), \\
&c_{1,3} = B_s\, ig(\alpha_9 - \eta\alpha_{13}) \\
&c_{2,3} = -c_d i(\alpha_5 - \mu\alpha_7) - c_d i(\alpha_5 - \mu\alpha_7) \\
&c_{2,2} = -c_d i(\alpha_5 - \mu\alpha_7) - Dig(\alpha_9 - \mu\alpha_{13}) \\
&c_{3,3} = -D_s ig(\alpha_9 - \mu\alpha_{13}) + A_s ig(\alpha_7 - \eta\alpha_9) \\
&\qquad - H_s(\alpha_9 - \eta\alpha_{13}) \\
&m_{1,1} = (\alpha_1 - \mu\alpha_3) I_0, \\
&m_{1,2} = (\alpha_7 - \mu\alpha_9) I_1, \\
&m_{1,3} = (\alpha_7 - \mu\alpha_9) J_1 \\
&m_{2,2} = (\alpha_5 - \mu\alpha_7) I_0 - (\alpha_7 - \mu\alpha_9) I_2, \\
&m_{2,3} = (\alpha_5 - \mu\alpha_7) I_0 - (\alpha_7 - \mu\alpha_9) J_2 \\
&m_{3,3} = (\alpha_5 - \mu\alpha_7) I_0 - (\alpha_7 - \mu\alpha_9) k_2
\end{aligned}
$$

In which

$$\alpha_1 = \int_0^L X'_m X'_m dx, \quad \alpha_3 = \int_0^L X'''_m X'_m dx \tag{46}$$

$$\alpha_5 = \int_0^L X_m X_m dx, \quad \alpha_7 = \int_0^L X''_m X_m dx, \quad \alpha_9 = \int_0^L X''''_m X_m dx \tag{47}$$

$$\alpha_{11} = \int_0^L X'''''_m X'_m dx, \quad \alpha_{13} = \int_0^L X''''''_m X_m dx \tag{48}$$

4. Numerical results and discussions

In this section the vibration characteristics of magneto-flexo-electrically actuated rotary porous (MFERP) nanobeam made of $BaTiO_3$ and $CoFe_2O_4$ are analyzed. The validity of the present study is proved by the means of comparing the frequencies of this model with those of Eltaher *et al*. (2012) for various nonlocal parameters as presented in Table 2.The length of nanobeam is considered to be L = 10 nm. Also, the dimensionless frequency and dimensionless form of viscoelastic parameters are adopted as follows

$$
\begin{aligned}
&\bar{\omega} = \omega L^2 \sqrt{\frac{\rho A}{EI}}, \qquad K_w = k_w \frac{L^4}{EI}, \qquad K_p = k_p \frac{L^2}{EI}, \\
&C = c_d \frac{L^2}{\sqrt{\rho A E I}}, \qquad \eta = \frac{g_0}{L^2}\sqrt{\frac{EI}{\rho A}}
\end{aligned} \tag{49}
$$

Table 2 Comparison of the frequency for power-law FG nanobeams

μ	p = 0.1		p = 0.5		p = 1	
	Eltaher *et al.* (2012)	Present	Eltaher *et al.* (2012)	Present	Eltaher *et al.* (2012)	Present
0	9.2129	9.1887	7.8061	7.7377	7.0904	6.9885
1	8.7889	8.7663	7.4458	7.3820	6.7631	6.6672
2	8.4166	8.3972	7.1312	7.0712	6.4774	6.3865
3	8.0887	8.0712	6.8533	6.7966	6.2251	6.1386

The influence of nonlocal parameter (μ) and strain gradient parameter (η) on the frequency response of MFERP nanobeam with L/h = 10, p = 0.5, ΔT = 30, ΔH = 1 and flexoelectric effect is illustrated in Figs. 2 and 3, respectively. It can be noticed from this figure that for the given damping coefficient, the imaginary Eigen frequency decrease with the increase in nonlocal parameter. Also, the critical damping coefficient increases with the reduction in the value of μ. However, a reverse trend is noticed with respect to the strain gradient parameter η. Meanwhile, for the real part of frequency, both μ and η is found to have a negligible influence.

Dimensionless Eigen frequency versus damping coefficient with various temperature and moisture environment of MFERP nanobeams with at K_w = 50, K_p = 10, G = 0.01, L/h = 10, p = 0.5, μ = 2 nm^2, η = 1 nm^2 affected by flexoelectricity is presented in Fig. 4. It can be noticed that the hygro-thermal environment has an important role in dimensionless vibration damping of MFERP nanobeams. As the hygrothermal load increases, at a constant damping coefficient, the imaginary frequency reduces. Further, improving the hygrothermal load (ΔT & ΔH) results in the reduction of critical damping coefficient.

Fig. 5 shows the dimensionless Eigen frequency with imaginary and real part of MFERP nanobeam under hygrothermal environment versus gradient index (p) for various damping coefficients with L/h = 10, K_w = 50, K_p = 10, ΔT = 30, ΔH = 1, η = 1 nm^2, μ = 2 nm^2 considering flexoelectric effect. It is highlighted in this figure that the value of imaginary part of the frequencies decreases by

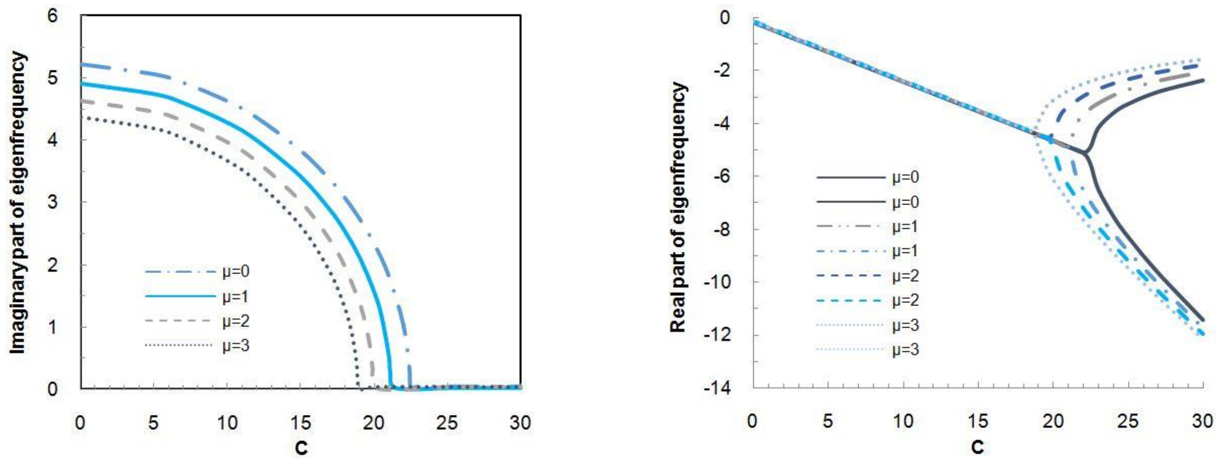

Fig. 2 The effect of nonlocal parameter on (a) imaginary part of eigen frequency (b) real part of eigen frequency (L/h = 20,p = 1, ΔT = 20, ΔH = 1, K_w = K_p = 0) of MFERP nanobeam

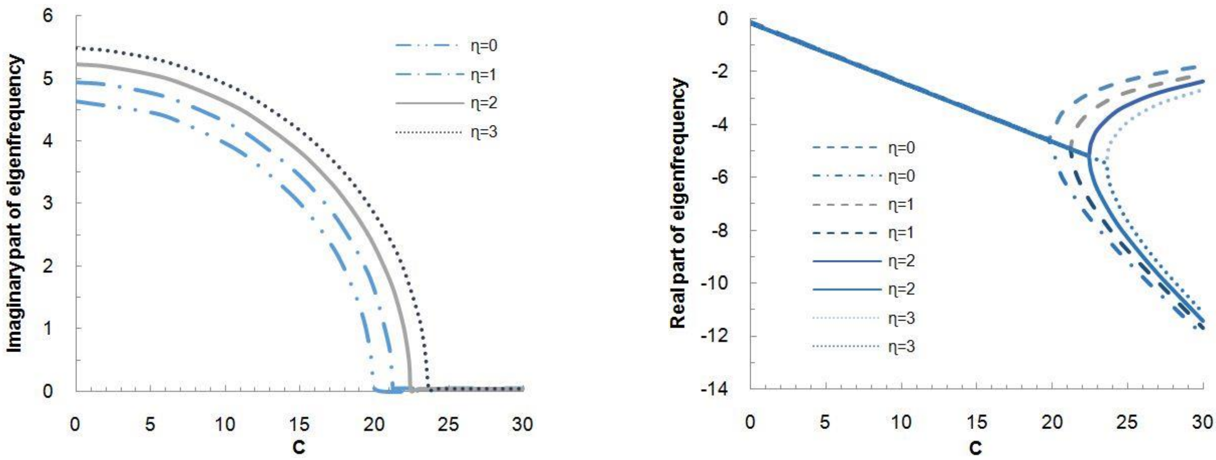

Fig. 3 The effect of length scale parameter on (a) imaginary part of eigen frequency (b) real part of eigen frequency (L/h = 20,p = 1, ΔT = 20, ΔH = 1, K_w = K_p = 0) of MFERP nanobeam

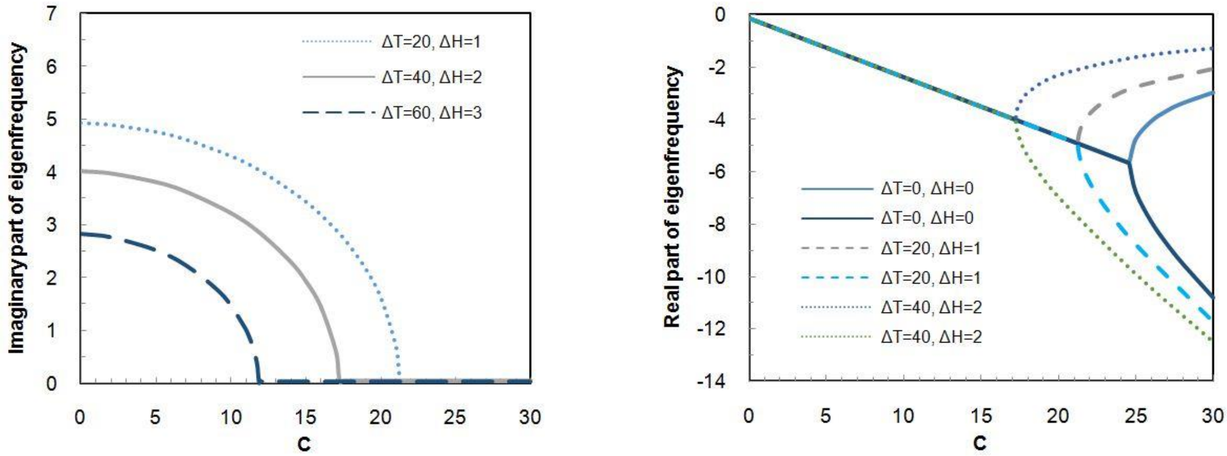

Fig. 4 The effect of Hygro-thermal loading on (a) imaginary part of eigen frequency, (b) real part of eigen frequency of MFERP nanobeam with damping coefficient (L/h = 10, ΔT = 20, ΔH = 1, K_w = 50, K_p = 10, μ = 2, h = 1)

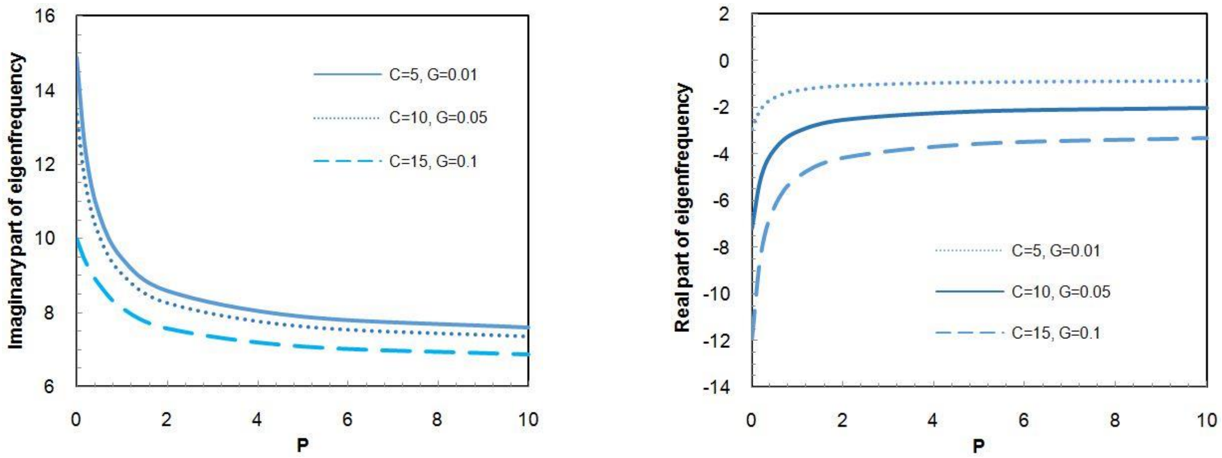

Fig. 5 The effect of material composition on (a) imaginary part of Eigen frequency, (b) real part of eigen frequency of MFERP nanobeam in hygrothermal environment (L/h = 20, ΔT = 20, ΔH = 1, K_w = 50, K_p = 10, μ = 2, h = 1)

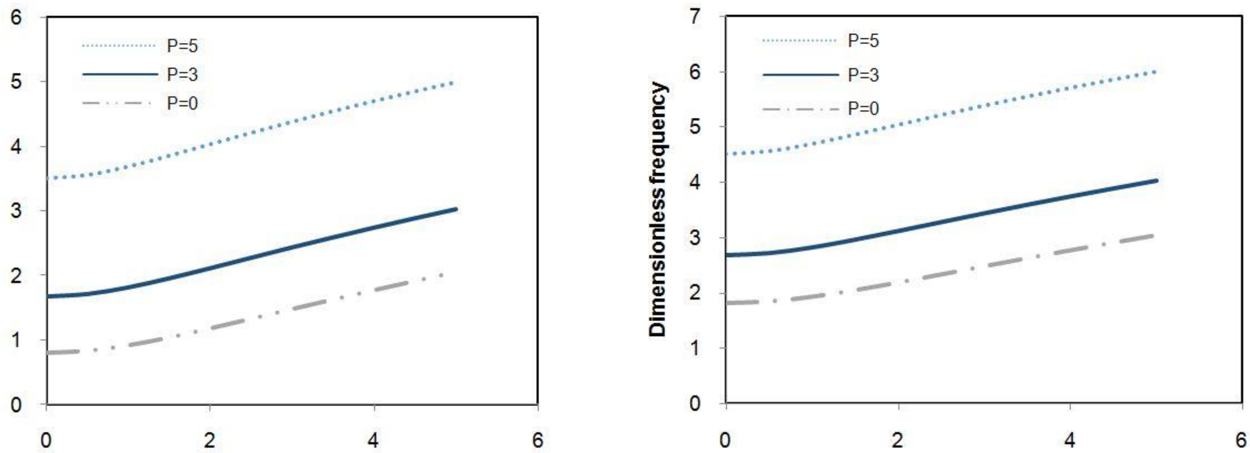

Fig. 6 Variation of dimensionless frequency of MFERP nanobeam versus length scale parameter for different gradient indices (L/h = 20, μ = 2 nm^2)

increasing the gradient index (p) whereas, the real part of the frequencies increases by increasing drastically at the initial values of gradient index. As the value of p further improves, the real part becomes almost constant. Also, it is witnessed that the lower magnitude of damping coefficients yields a higher value of frequencies in contrast to the higher

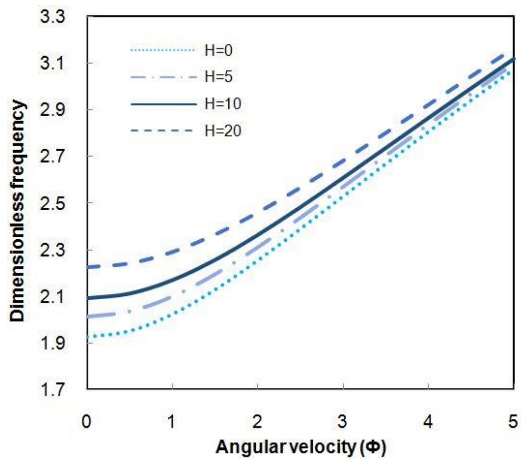

Fig. 7 Variation of first dimensionless frequency of MFERP nanobeam versus angular velocity for different magnetic field intensities (L/h = 30, μ = 2 nm^2, p = 1)

damping coefficients.

The effects of Winkler and Pasternak parameters on the variations of the first dimensionless frequency of MFERP nanobeams versus power-law exponent for different electric voltages at L/h = 10 and p = 1 are presented in Fig. 6. It is seen that for all values of elastic foundation constants the non-dimensional frequency reduces with the increase of power-law exponent.

The variation of dimensionless natural frequencies of MFERP nanobeam with respect angular velocity at constant slenderness ratio L/h = 10 and nonlocal parameter β = 2 nm^2 is presented in Fig. 7. It can be witnessed from this figure that the higher angular velocity has a predominant influence on the dimensionless frequency of MFERP nanobeam. In addition an increment in the magnetic field raises the frequency of the MFERP nanobeams.

The variations of dimensionless frequency versus gradient index for MFERP nanobeam with different porosity volume are examined at μ = 1, Φ = 1 Grad/s, $\mu = 0.1 \times 10^9$ are presented in Fig. 8. From the figure it is

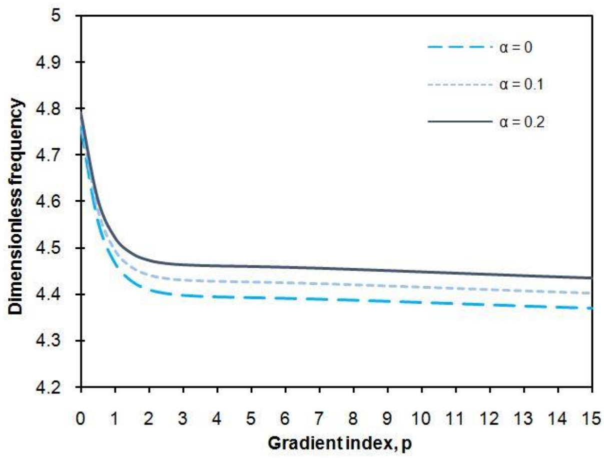

Fig. 8 The effect of porosity volume on frequency response of MFERP nanobeam versus gradient index (μ = 1, Φ = 1 Grad/s, $\mu = 0.1 \times 10^9$)

evident that as the gradient index improves, the dimensionless frequencies reduce drastically. In addition higher value of α has a significant effect on the frequency of MFERP nanobeams.

5. Conclusions

In this paper, the frequency response of MFERP nanobeams under hygrothermal environment has been evaluated incorporating nonlocal strain gradient theory beam model. It can be highlighted that the proposed model tailors both nonlocal elasticity theory and strain gradient theory to capture the size effects much accurately. A nonlocal stress parameter as well as a length scale parameter is employed to involve both stiffness-softening and stiffness-hardening influences on vibration of MFERP nanobeams. The governing differential equations of motion are derived by using Hamilton's principle and an analytical solution is employed to solve the equations for S-S boundary conditions. The results reveal that the nonlocal parameter has a detrimental effect on the frequency whereas the length scale parameter improves it. Increasing the hygrothermal load reduces the critical damping coefficient of MFERP nanobeams. The magnitude of both real and imaginary eigen frequencies reduces by increasing gradient index (p), especially at lower gradient indexes. Meanwhile, it is witnessed that the frequency response of MFERP nanobeam increases with a higher value of applied magnetic field and porosity volume.

References

Ansari, R., Pourashraf, T. and Gholami, R. (2015), "An exact solution for the nonlinear forced vibration of functionally graded nanobeams in thermal environment based on surface elasticity theory", *Thin-Wall. Struct.*, **93**, 169-176. https://doi.org/10.1016/j.tws.2015.03.013

Arefi, M. and Zenkour, A.M. (2016), "A simplified shear and normal deformations nonlocal theory for bending of functionally graded piezomagnetic sandwich nanobeams in magneto-thermo-electric environment", *J. Sandw. Struct. Mater.*, **18**(5), 624-651. https://doi.org/10.1177/1099636216652581

Civalek, Ö. and Demir, Ç. (2011), "Bending analysis of microtubules using nonlocal Euler–Bernoulli beam theory", *Appl. Math. Model.*, **35**(5), 2053-2067. https://doi.org/10.1016/j.apm.2010.11.004

Ebrahimi, F. and Barati, M.R. (2016a), "Dynamic modeling of a thermo–piezo-electrically actuated nanosize beam subjected to a magnetic field", *Appl. Phys. A*, **122**(4), 451. https://doi.org/10.1007/s00339-016-0001-3

Ebrahimi, F. and Barati, M.R. (2016b), "Electromechanical buckling behavior of smart piezoelectrically actuated higher-order size-dependent graded nanoscale beams in thermal environment", *Int. J. Smart Nano Mater.*, **7**(2), 69-90. https://doi.org/10.1080/19475411.2016.1191556

Ebrahimi, F. and Barati, M.R. (2016c), "An exact solution for buckling analysis of embedded piezoelectro-magnetically actuated nanoscale beams", *Adv. Nano Res., Int. J.*, **4**(2), 65-84. http://dx.doi.org/10.12989/anr.2016.4.2.065

Ebrahimi, F. and Barati, M.R. (2016d), "Vibration analysis of smart piezoelectrically actuated nanobeams subjected to magneto-electrical field in thermal environment", *J. Vib. Control*,

1077546316646239.
https://doi.org/10.1177/1077546316646239
Ebrahimi, F. and Barati, M.R. (2017), "Buckling analysis of nonlocal third-order shear deformable functionally graded piezoelectric nanobeams embedded in elastic medium", *J. Brazil. Soc. Mech. Sci. Eng.*, **39**(3), 937-952.
https://doi.org/10.1007/s40430-016-0551-5
Eltaher, M.A., Emam, S.A. and Mahmoud, F.F. (2012), "Free vibration analysis of functionally graded size-dependent nanobeams", *Appl. Math. Computat.*, **218**(14), 7406-7420.
https://doi.org/10.1016/j.amc.2011.12.090
Eringen, A.C. (1968), "Mechanics of micromorphic continua", In: *Mechanics of generalized continua*, Springer, Berlin, Heidelberg, Germany, pp. 18-35.
Eringen, A. (1972), "Nonlocal polar elastic continua", *Int. J. Eng. Sci.*, **10**, 1-16. https://doi.org/10.1016/0020-7225(72)90070-5
Ghorbanpour Arani, A. and Zamani, M.H. (2017), "Investigation of electric field effect on size-dependent bending analysis of functionally graded porous shear and normal deformable sandwich nanoplate on silica Aerogel foundation", *J. Sandw. Struct. Mater.*, 1099636217721405.
https://doi.org/10.1177/1099636217721405
Ke, L.L. and Wang, Y.S. (2014), "Free vibration of size-dependent magneto-electro-elastic nanobeams based on the nonlocal theory", *Physica E: Low-dimens. Syst. Nanostruct.*, **63**, 52-61.
https://doi.org/10.1016/j.physe.2014.05.002
Kiani, Y., Rezaei, M., Taheri, S. and Eslami, M.R. (2011), "Thermo-electrical buckling of piezoelectric functionally graded material Timoshenko beams", *Int. J. Mech. Mater. Des.*, **7**(3), 185-197. https://doi.org/10.1007/s10999-011-9158-2
Murmu, T. and Pradhan, S.C. (2009), "Buckling analysis of a single-walled carbon nanotube embedded in an elastic medium based on nonlocal elasticity and Timoshenko beam theory and using DQM", *Physica E: Low-dimens. Syst. Nanostruct.*, **41**(7), 1232-1239. https://doi.org/10.1016/j.physe.2009.02.004
Peddieson, J., Buchanan, G.R. and McNitt, R.P. (2003), "Application of nonlocal continuum models to nano-technology", *Int. J. Eng. Sci.*, **41**(3), 305-312.
https://doi.org/10.1016/S0020-7225(02)00210-0
Rahmani, O. and Jandaghian, A.A. (2015), "Buckling analysis of functionally graded nanobeams based on a nonlocal third-order shear deformation theory", *Appl. Phys. A*, **119**(3), 1019-1032.
https://doi.org/10.1007/s00339-015-9061-z
Roque, C.M.C., Ferreira, A.J.M. and Reddy, J.N. (2011), "Analysis of Timoshenko nanobeams with a nonlocal formulation and meshless method", *Int. J. Eng. Sci.*, **49**(9), 976-984. https://doi.org/10.1016/j.ijengsci.2011.05.010
Şimşek, M. and Yurtcu, H.H. (2013), "Analytical solutions for bending and buckling of functionally graded nanobeams based on the nonlocal Timoshenko beam theory", *Compos. Struct.*, **97**, 378-386. https://doi.org/10.1016/j.compstruct.2012.10.038
Wang, Q. (2005), "Wave propagation in carbon nanotubes via nonlocal continuum mechanics", *J. Appl. Phys.*, **98**(12), 124301.
https://doi.org/10.1063/1.2141648
Wang, C.M., Kitipornchai, S., Lim, C.W. and Eisenberger, M. (2008), "Beam bending solutions based on nonlocal Timoshenko beam theory", *J. Eng. Mech.*, **134**(6), 475-481.
https://doi.org/10.1061/(ASCE)0733-9399(2008)134:6(475)
Yang, J., Ke, L.L. and Kitipornchai, S. (2010), "Nonlinear free vibration of single-walled carbon nanotubes using nonlocal Timoshenko beam theory", *Physica E: Low-dimens. Syst. Nanostruct.*, **42**(5), 1727-1735.
https://doi.org/10.1016/j.physe.2010.01.035
Zenkour, A.M. and Sobhy, M. (2013), "Nonlocal elasticity theory for thermal buckling of nanoplates lying on Winkler–Pasternak elastic substrate medium", *Physica E: Low-dimens. Syst. Nanostruct.*, **53**, 251-259.
https://doi.org/10.1016/j.physe.2013.04.022

JL